COMPUTATION OF EFFECTIVE BENDING STIFFNESS OF RC TELECOMMUNICATION TOWER BASED ON EXPERIMENTAL DATA

M. A. Silva[(1)], J. S. Arora[(2)] and R. M. L. R. F. Brasil[(3)]

(1) - Department of Structural and Foundations Engineering of Polytechnic School of The University of Sao Paulo, PEF/EPUSP – Pos-Doctoral Student
R. Parnamirim, 97, A 24, CEP 05.331-020, Sao Paulo -SP., Brazil
E-mail: m_araujo_silva@uol.com.br
- Scac Fundações e Estruturas Ltda., Structural Technical Division – Project Manager

(2) - F. Wendell Miller Distinguished Professor of Engineering, The University of Iowa
Associate Director, Virtual Soldier Research (VSR) Program/CCAD
4110 SC/Eng/UIowa, Iowa City, IA 52242
E-mail: jasbir-arora@uiowa.edu

(3) - Department of Structural and Foundations Engineering of Polytechnic School of The University of Sao Paulo, PEF/EPUSP – Associated Professor
Cx. Postal 61548, CEP 05.424-970, Sao Paulo -SP., Brazil
E-mail: rmlrdfbr@usp.br

Abstract

We present some results of the application of optimization techniques to experimental data for the determination of the effective bending stiffness of cross-sections of reinforced concrete (RC) structures. The objective is to determine parameters of unstressed sections for the correct computation of the displacements of these structures and possible applications on structural failure theory. The experimental data from tests with 30 and 40 *m* long RC telecommunication towers, having circular cross-section with 50 *cm* diameter for the 30 *m* structure and 60 *cm* diameter for the 40 *m* structure, are used. For cross-sections along the axis of the structure, the effective stiffness equation is derived. To accomplish the structural analysis, the structures are discretized and the differential equation of the elastic line integrated to obtain the rotations and displacements. Optimization problems are defined so that the objective functions are the approximation errors, while the design variables are the coefficients of the effective bending stiffness equations of the cross-sections. Two different formulations are used to compute the effective stiffness. The first one gives one equation for each node section and the other formulation provides only one equation for the whole structure. The effective stiffness is presented in graphs as function of a ratio between the characteristic bending moment and the ultimate moment of the cross-section. The sections where the largest stiffness loss are obtained were the sections that indeed collapsed in real similar structures. Directions for future research are presented.

Keywords: Effective bending stiffness; experimental results; large displacements; reinforced concrete; structural optimization.

1 Introduction and Motivation

One of the pertinent verifications in structural design is to check if the computed displacements are inside certain limits specified by codes. In RC structures, in function of the specificities of this product, such as cracking and cross-section stiffness reduction, this calculation becomes sometimes imprecise and, in those cases, the installed structures may undergo displacements that are larger than the predicted design displacement. In structural design, the cracking phenomena in RC structures are interpreted as a physical non-linearity. In other words, the stiffness depends mainly on the bending moment value.

As a contribution to the studies found in literature on the determination of effective stiffness in RC cross-sections, we present two different formulations to compute the effective bending stiffness of RC telecommunication tower as function of the bending moment value in a certain section. The methodology of this work is based on comparing the displacements measured in experimental work in sample RC structures with numerical data obtained integrating the elastic line. The quadratic error between the real measured and those provided by the elastic line integration is minimized using optimization techniques. The objective function is the quadratic error, while the design variables are the coefficients of trial effective stiffness equations for each section. Constraints are imposed on the maximum and minimum values of the effective stiffness.

As a consequence of our study, it may be possible to forecast more precisely the displacements of the RC beams. Possible applications of the results are also in prediction of structural collapse and nonlinear structural analysis.

2 A Brief Review of Literature

The two main tools to be used in this work are concepts of RC structures design and optimization techniques. For the RC analysis we adopt usual Brazilian methods, as presented by Brazilian National Codes NBR-6118-03 (ABNT [3]). A review of the specialized literature indicates that the effective stiffness of a RC cross-section of a beam depends on the bending moment value, as well as the arrangement of the reinforcement and the properties of material components. An equation proposed by Dan E. Branson in 1963 (Branson [6]) for the calculation of the effective stiffness was incorporated in ACI-318-71 (ACI [4]) and recently in NBR-6118-03 (ABNT [3]). Several researchers and designers have used the Branson equation to compute the displacements of RC beams. In this work, inspired in Branson's, we present another formulation to obtain the equations to represent the effective bending stiffness as function of the bending moment, using optimization techniques.

With respect to the optimization process, we use the Augmented Lagrangian Method (Chahande and Arora [9]). To render the constrained optimization problem into an unconstrained optimization problem, a Lagrangian functional is created. The

objective and constraint functions are associated to Lagrange multipliers and penalty parameters. A sequence of Lagrangians is developed by properly varying the multipliers and penalty parameters. The minimum value of the Lagrangian function converges to the minimum of the optimization problem with constraints. In the cases analyzed in this work, the coefficients of the effective stiffness equations of the chosen cross-sections are the design variables for the error minimization problem. The error between the numerical and displacements measured in tests is the objective function, while the maximum and minimum values of the effective stiffness are the constraints. The line search algorithms we need to use in the process demand both the objective and constraints functions to be differentiable with respect to the design variables. In a certain stage of the calculation process, the method of the least squares is used (Arora [5]).

Silva and Brasil [10, 11] and Brasil and Silva [7, 8] used optimization techniques to compute the effective bending stiffness of slender RC structures as function of the bending moment value was. They presented results of experiments performed in several sample structures. They defined optimization problems where the design variables were the coefficients of some trial effective stiffness equations. The objective function was the quadratic error between the displacements measured in the experiments and those given by the integration of neutral line equation. They solved the optimization problems and obtained the effective stiffness equations for several kinds of structures. They considered several different functions to represent the effective stiffness parameter such as polynomial and trigonometric equations. In a paper by Silva and Brasil [11] a nonlinear dynamic analysis based on experimental results of a RC telecommunication tower was carried out using the discrete dynamic model given by NBR-6123-87 (ABNT [1]). First, they described some tests accomplished and results obtained for similar structures (Silva and Brasil [10]). They considered two different equations to represent the effective stiffness parameter: one a linear one and another a cubic equation. Once the effective stiffness equations and other information are known, they accomplished a nonlinear static analysis, under the mean wind velocity, considering the effective bending stiffness as a function of the bending moment value in each iteration of the P-Delta method. Considering the effective stiffness obtained in the final iteration of the P-Delta method they applied the discrete model given in NBR-6123-87 (ABNT [1]) to accomplish the dynamic analysis considering the floating wind velocity. They considered that the structure, under the floating wind velocity, vibrates around the equilibrium position given by the mean wind velocity and P-Delta method. Finally, they computed the sum of nonlinear static and linear dynamic bending moments. They compared the values obtained from dynamic analysis with those obtained from linear static analysis and those obtained in experimental work. The displacement values obtained in the proposed dynamic analysis were up to 40 % lager than those given by a static linear analysis. The tests results showed that the cross-section ultimate moment is up to 40 % larger than that given by NBR-6118-03 (ABNT [3]).

3 Experimental Results

A series of tests were conducted at the plant of SCAC Fundações e Estruturas Ltda. at São Paulo, Brazil. They were carried out on two centrifuged RC structures 30 and 40 *m* long, of circular cross-section with 50 *cm* diameter for the 30 *m* long structure and 60 *cm* for the 40 *m* long structure. The thicknesses vary from 8 to 15 *cm*. The 40 *m* long structure presented 3 *m* of embedment while the 30 *m* presented 2 *m*. The geometrical and steel area data are shown in Table 1 for the 30 *m* long structure and Table 2 for the 40 *m* long structure. In those tables we have, in sequence, the sections numbering, the height above ground, the external diameter (ϕ_{ext}), the thickness (thick.), the total area of cross-section (A_{total}), the total longitudinal steel area (A_s), the total moment of inertia of cross-section (I_{total}), including the steel and concrete inertia, and the minimum value to be adopted by the parameter of effective stiffness *w* (w_s). The 30 *m* structure was designed and fabricated in three modules with lengths of 10 *m* for top module and 11 *m* for others (Fig. 1), while the 40 *m* was designed and fabricated in four modules with lengths of 10 *m* for top module and 11 *m* for others (Fig. 2). Flanges installed at the extremities of them bolt these modules.

Table 1 -- Geometrical and steel area characteristics of the 30 *m* above ground long structure

Section	Height (m)	ϕext (cm)	thick. (cm)	A total (cm4)	Ic total (cm4)	As (cm2)	Itotal (cm4)	ws
30	30,00	50,00	9,56	1215	262161	18,1	283414	0,07
29	29,00	50,00	9,56	1215	262161	18,1	283414	0,07
28	28,00	50,00	9,56	1215	262161	18,1	283414	0,07
27	27,00	50,00	9,56	1215	262161	18,1	283414	0,07
26	26,00	50,00	9,56	1215	262161	18,1	283414	0,07
25	25,00	50,00	9,56	1215	262161	18,1	283414	0,07
24	24,00	50,00	9,56	1215	262161	18,1	283414	0,07
23	23,00	50,00	9,56	1215	262161	18,1	283414	0,07
22	22,00	50,00	9,56	1215	262161	18,1	283414	0,07
21	21,00	50,00	9,56	1215	262161	18,1	283414	0,07
20	20,00	50,00	12,66	1485	288584	18,0	309762	0,07
19	19,00	50,00	12,75	1492	289110	42,2	338005	0,14
18	18,00	50,00	12,84	1499	289624	48,3	345546	0,16
17	17,00	50,00	11,16	1362	277980	26,1	308271	0,10
16	16,00	50,00	11,16	1362	277980	28,1	310601	0,11
15	15,00	50,00	11,16	1362	277980	30,2	312931	0,11
14	14,00	50,00	11,16	1362	277980	30,2	312931	0,11
13	13,00	50,00	11,16	1362	277980	32,2	315261	0,12
12	12,00	50,00	11,16	1362	277980	34,2	317591	0,12
11	11,00	50,00	11,16	1362	277980	36,2	319921	0,13
10	10,00	50,00	11,16	1362	277980	40,2	324582	0,14
9	9,00	50,00	12,84	1499	289624	80,4	381128	0,24
8	8,00	50,00	14,97	1647	298832	87,3	398199	0,25
7	7,00	50,00	17,09	1767	303722	94,2	410952	0,26
6	6,00	50,00	12,29	1456	286300	50,3	343490	0,17
5	5,00	50,00	12,29	1456	286300	53,4	347064	0,18
4	4,00	50,00	12,29	1456	286300	53,4	347064	0,18
3	3,00	50,00	12,29	1456	286300	56,5	350638	0,18
2	2,00	50,00	12,29	1456	286300	59,7	354213	0,19
1	1,00	50,00	12,29	1456	286300	62,8	357787	0,20
0	0,00	50,00	12,29	1456	286300	62,8	357787	0,20

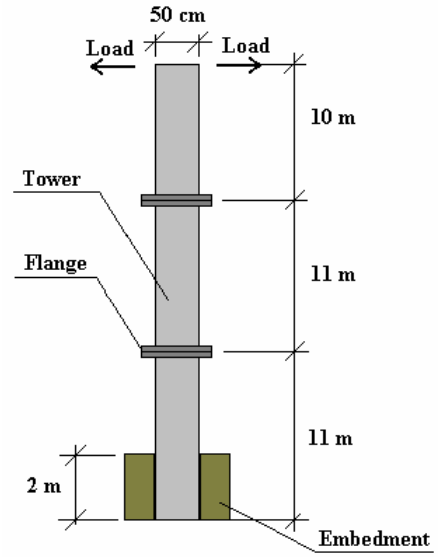

Fig. 1 -- Outline of the 30 *m* long structure assembly

Once the structural designs were known, an appropriate planning of the several tests was prepared. The tests had the objective to evaluate the structures at the utilization limit state and ultimate limit state. The following parameters were measured during the tests: applied loads; displacements; occurrence and opening of cracks; residual displacements. The tests were performed with the structures in horizontal position. Figs. 1 and 2 illustrate the test rig used for the 30 *m* and 40 *m* long structures respectively. The tests for the 40 *m* structure were done in two stages: the first one with the embedment at 7 *m* from base; the second one with the structure without the top module and the embedment at 3 *m* from base.

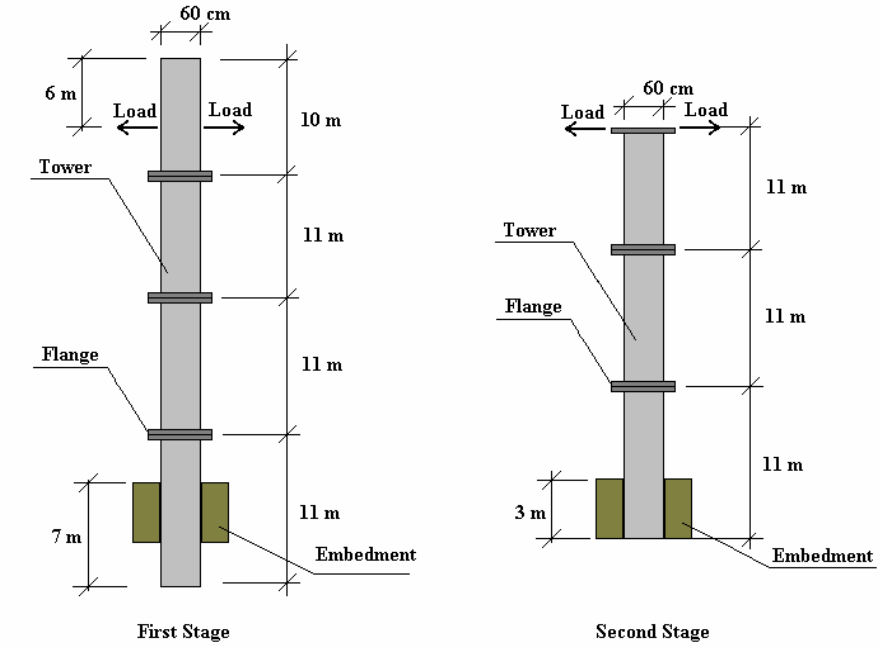

Fig. 2 -- Outline of the 40 *m* long structure assembly

Table 2 -- Geometrical and steel area characteristics of the 40 *m* above ground long structure

Section	Height (m)	ϕext (cm)	thick. (cm)	A total (cm4)	As (cm2)	Itotal (cm4)	ws
40	40,00	60,00	9,61	1521	24,5	544293	0,08
39	39,00	60,00	9,61	1521	24,5	544293	0,08
38	38,00	60,00	9,61	1521	24,5	544293	0,08
37	37,00	60,00	9,61	1521	24,5	544293	0,08
36	36,00	60,00	9,61	1521	24,5	544293	0,08
35	35,00	60,00	9,61	1521	24,5	544293	0,08
34	34,00	60,00	9,61	1521	24,5	544293	0,08
33	33,00	60,00	9,61	1521	24,5	544293	0,08
32	32,00	60,00	9,61	1521	24,5	544293	0,08
31	31,00	60,00	13,41	1963	24,5	620555	0,07
30	30,00	60,00	12,37	1850	30,2	613428	0,09
29	29,00	60,00	11,32	1731	30,2	593758	0,09
28	28,00	60,00	11,19	1716	30,2	591068	0,09
27	27,00	60,00	11,19	1716	30,2	591068	0,09
26	26,00	60,00	11,19	1716	30,2	591068	0,09
25	25,00	60,00	11,19	1716	32,2	594616	0,10
24	24,00	60,00	11,19	1716	34,2	598163	0,10
23	23,00	60,00	11,19	1716	36,2	601711	0,11
22	22,00	60,00	11,19	1716	38,2	605259	0,11
21	21,00	60,00	11,19	1716	40,2	608807	0,12
20	20,00	60,00	13,51	1973	40,2	649055	0,11
19	19,00	60,00	14,91	2112	47,1	677310	0,12
18	18,00	60,00	16,30	2238	47,1	690420	0,12
17	17,00	60,00	13,01	1921	50,3	658106	0,13
16	16,00	60,00	13,01	1921	50,3	658106	0,13
15	15,00	60,00	13,01	1921	53,4	663567	0,14
14	14,00	60,00	13,01	1921	56,5	669028	0,15
13	13,00	60,00	13,01	1921	59,7	674489	0,15
12	12,00	60,00	13,01	1921	59,7	674489	0,15
11	11,00	60,00	13,01	1921	62,8	679950	0,16
10	10,00	60,00	13,01	1921	69,1	690872	0,17
9	9,00	60,00	16,30	2238	69,1	728648	0,16
8	8,00	60,00	16,44	2249	73,6	735192	0,17
7	7,00	60,00	16,57	2261	73,6	736235	0,17
6	6,00	60,00	14,40	2063	78,5	723645	0,19
5	5,00	60,00	14,40	2063	78,5	723645	0,19
4	4,00	60,00	14,40	2063	83,4	732019	0,19
3	3,00	60,00	14,40	2063	83,4	732019	0,19
2	2,00	60,00	14,40	2063	83,4	732019	0,19
1	1,00	60,00	17,69	2351	83,4	760498	0,19
0	0,00	60,00	17,69	2351	83,4	760498	0,19

Static loads were applied to the pole tip to produce bending moment and shear load along its axis. The loads were applied in the perpendicular direction to the structure axis. A stretched steel wire installed right above the structure materialized a fixed reference axis. Starting from the steel wire the displacements were measured at every 5 *m* of increment along the pole length. Movable supports were installed along the length of the structure to minimize forces due to self-weight and friction with ground. The structure supports were designed to a load three times larger than its Brazilian Code predicted ultimate load. The apparatus was also long enough to provide appropriate embedment.

Table 3 -- Loads and measured displacements of the 30 m above ground long structure

Step	Load (N)		Displacements (cm)						
	Value	Orientation	30m	29m	25m	20m	15m	10m	5m
1	600	right	0,1	0,0	0,0	0,0	0,0	0,0	0,0
2	600	left	0,2	0,2	0,0	0,0	0,0	0,0	0,0
3	2500	left	20,1	18,8	14,8	10,0	5,8	2,9	0,6
4	3600	left	35,0	32,8	25,9	17,3	10,0	5,2	1,5
5	5100	left	46,7	44,1	34,4	23,0	13,6	6,8	1,9
6	7600	right	93,0	87,9	68,0	45,4	26,3	12,6	4,1
7	7600	left	100,5	95,2	74,9	51,1	30,7	15,7	4,7
8	10200	right	163,1	154,7	120,4	80,9	47,8	23,1	7,2
9	12700	left	243,6	231,9	184,7	129,6	80,9	48,7	14,9
10	12700	right	214,7	203,2	157,1	104,2	60,1	28,1	8,8

Once the structure was appropriately installed, along with the systems of load application and data acquisition, the loads were first applied from left to right and then from right to left and so on (Figs. 1, 2). Loads were applied gradually and after their stabilization the measured parameters were read. The intensity of the applied loads started at 5% of the ultimate Code based top load and increased gradually along the test stages to reach the collapse load of the structures. The characteristics of the structures, as well as the parameters values measured in the tests, mainly those related to the displacements and applied loads, are used in numerical simulations later. The tests were performed in one stage for 30 *m* structure and, for the 40 *m* structure, in two stages: the first one with the embedment at 7 *m* from base; the second one with the structure without the top module and the embedment at 3 *m* from base. The loads applied and displacements measured in tests are shown in Tables 3 and 4.

Table 4 -- Loads and measured displacements of the 40 *m* above ground long structure

STAGE 1								
Step	Load (N)		Displacements (cm)					
	Value	Orientation	30m	25m	20m	15m	10m	5m
1	2100	right	3,3	2,3	1,1	0,2	0,1	0,0
2	2100	left	2,7	1,6	1,0	0,6	0,2	0,0
3	4200	left	14,2	10,1	6,8	3,8	2,3	1,0
4	4200	right	6,9	4,4	3,1	1,1	0,6	0,3
5	6400	right	19,7	14,0	9,4	5,3	2,8	0,8
6	6400	left	32,2	23,5	15,5	11,8	4,2	1,0
7	4600	right	16,3	12,0	8,4	5,4	2,6	0,7
8	4600	left	24,8	18,1	11,8	7,0	3,3	0,6
9	7000	left	33,0	24,1	16,4	8,3	4,1	1,0
10	7000	right	26,6	19,4	13,0	8,2	3,5	1,3
11	9200	right	43,5	32,3	21,5	13,0	6,2	2,2
12	9200	left	55,3	41,0	28,0	16,2	7,5	2,3
13	13900	left	120,0	89,9	61,6	37,3	17,9	6,0
14	13900	right	69,4	50,6	33,1	19,0	8,2	2,0
15	18500	right	118,7	86,3	56,3	32,8	14,9	4,1
16	18500	left	189,9	142,2	196,5	59,1	28,9	9,5
17	23100	right	161,5	117,3	76,9	45,2	20,8	6,2
18	23100	right	207,5	153,2	102,1	61,2	28,6	8,8
STAGE 2								
Step	Load (N)		Displacements (cm)					
	Value	Orientation	30m	25m	20m	15m	10m	5m
19	8600	left	47,2	34,3	22,9	12,9	6,1	1,6
20	8600	right	39,9	28,5	18,4	10,0	3,9	1,0
21	28200	right	261,5	194,2	133,0	80,7	40,4	13,7
22	33800	right	396,2	297,8	207,4	129,3	66,3	22,8

4 Determination of Effective Stiffness

4.1 First Formulation – One Equation for Each Section

This formulation provides one equation for each section. So for one 30 *m* long structure, discretized in each one meter, it provides 31 equations. This formulation is very important because it can give information specifically about the behavior of one given section. For example, Silva and Brasil [10] and Brasil and Silva [8] showed that during a failure test in a 30 m long structure, the section that present the largest loss of stiffness is the section that really collapse when the structure failure occurs.

Consider the differential neutral line equation given by

$$EI_{EF}(z)v(z)'' = -M_k(z)\,, \tag{1}$$

where $I_{EF}(z)$, $v(z)$ and $M_k(z)$ are respectively the effective moment of inertia, the displacement and the characteristic bending moment of a transverse section with abscissa z. The concrete elasticity modulus (E = 41,4 *GPa*) is calculated as a function of f_{ck} = 45 *MPa* (characteristic compressive resistance of 28 days old concrete), as given by NBR-6118-78 (ABNT [2]) Brazilian Code. In the cases analyzed in this work, boundary conditions are $v(0) = 0$ and $v'(0) = 0$. The one-dimensional domain is the set $D = \{z \in \Re \mid 0 \le z \le L\}$. Dividing D in n segments, the discretized structure domain will now be $D_n = \{z \in \Re \mid z = z_0, \quad z_1, \quad \cdots \quad z_i, \quad \cdots \quad z_n\}$. For each point z_i, $i > 0$, in this domain we compute $v_i = v(z_i)$, $v'_i = v'(z_i)$ and $v''_i = v''(z_i)$ using the following integration scheme:

$$\begin{aligned} v''_i &= -\frac{M_k(z_i)}{EI_{EF}(z_i)} \\ v'_i &= v'_{i-1} + \frac{v''_i + v''_{i-1}}{2}h \\ v_i &= v_{i-1} + \frac{v'_i + v'_{i-1}}{2}h \end{aligned} \tag{2}$$

where $h = z_i - z_{i\text{-}1}$. For each section z_i we consider the value of the effective moment of inertia

$$I_{EF}(z_i) = w_i\, I(z_i), \tag{3}$$

where $I(z_i)$ is the total homogenized moment of inertia (including concrete and homogenized steel) of the cross section z_i, and w_i is the portion of $I(z_i)$ that will actually resist the bending moment at each section. The total bending stiffness is

defined as $EI(z_i)$, while the effective bending stiffness is $EI_{EF}(z_i)$. As I_{EF} depends on z_i and w_i,, from now on we will denote $I_{EF}(z_i,w_i)$. As a consequence, $v_i = v(z_i,\boldsymbol{w})$, where $\boldsymbol{w} = \begin{bmatrix} w_0 & w_1 & \cdots & w_i & \cdots & w_n \end{bmatrix}^T$.

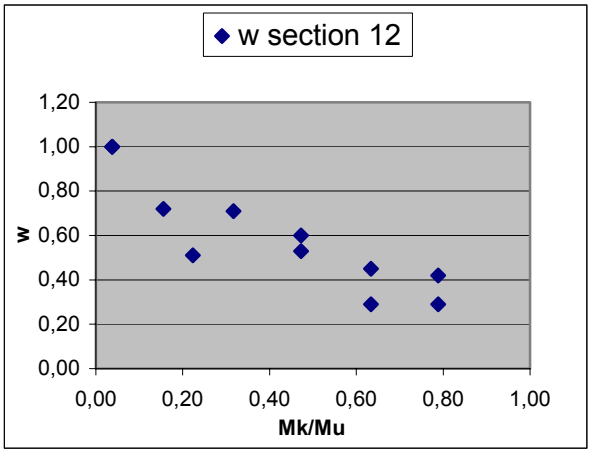

Fig. 3 -- Points obtained for section 12 for the 30 *m* long structure

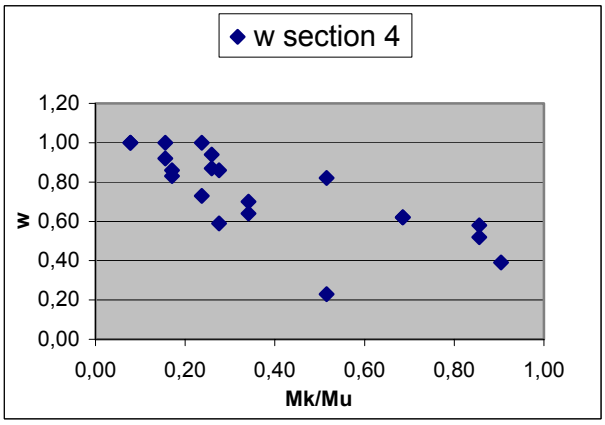

Fig. 4 -- Points obtained for section 6 for the 40 *m* long structure

Consider that the test described in Section 3 has been accomplished in a certain structure. During the test the real displacements $v_r(x_i)$ were measured in some *m* sections of the structure under a certain loading. The absolute quadratic approximation error between the displacements given by Eq. (2) and those measured during the tests is the sum of *m* terms:

$$E_q(\boldsymbol{w}) = \frac{1}{2}\sum_i \left[v(z_i,\boldsymbol{w}) - v_r(z_i)\right]^2 \qquad (4)$$

We can formulate the following optimization problem. Determine $\boldsymbol{w} \in \Re^{n+1}$ that minimize the objective function

$$f(\boldsymbol{w}) = E_q(\boldsymbol{w}), \tag{5}$$

subjected to constrains:

$$w_s(z_i) \le w_i \le 1, \quad \text{para} \quad i = 0, 1, ..., n \tag{6}$$

where $w_s(z_i) = E_s I_s(z_i)/EI(z_i)$ (Tables 1, 2), where I_s and E_s = 210 *GPa* are, respectively, the steel moment of inertia and the elasticity modulus of the longitudinal reinforcement in section *i*. Solving the problem given by Eq. (5) and (6), we obtain the stiffness ratios *w* for a certain loading. The same calculations for all loading hypotheses will render a relationship between w_i and $M_k(z_i)/M_u(z_i)$, where M_u is the ultimate Code based moment computed according to NBR-6118-03 (ABNT [3]) Brazilian code, and

$$x = M_k(z_i)/M_u(z_i), \tag{7}$$

is the bending moment value in section z_i. As we noted earlier, we accomplished this analysis for 30 and 40 *m* long structures. The loads were applied from right to left and left to right, according to Tables 3 and 4. The structures were discretized in each one meter. Thus, the domains are $D_{30} = \{z \in \Re \mid z = 0, \quad 1, \quad \cdots, \quad 30\}$ and $D_{40} = \{z \in \Re \mid z = 0, \quad 1, \quad \cdots, \quad 40\}$, in meters. The points results for sections i = 12 for the 30 *m* long structure and i = 4 for the 40 *m* long structure are shown in Figs. 3 and 4 respectively.

Table 5 -- Values of *a*, *b*, *c* and *d* for sections solicited up to $0.8M_u$, for the 30 *m* long structure

Coefficients		Sections																Mean
		0	1	2	3	4	5	6	10	11	12	13	14	15	16	17	21	
LINE	a	-0,8	-0,9	-1,1	-1,1	-0,6	-0,6	-0,6	-0,6	-0,7	-0,8	-0,8	-0,8	-0,8	-0,9	-1,1	-0,6	**-0,8**
	b	1,0	0,9	1,0	1,0	0,9	0,9	0,9	0,9	0,9	0,9	0,9	0,9	0,9	0,9	0,9	0,9	**0,9**
	Error	0,05	1,42	0,33	0,17	0,50	0,39	0,43	0,79	0,74	0,61	0,51	0,60	0,73	1,02	2,54	1,17	**0,75**
QUADRATIC	a	0,1	2,0	0,8	0,8	1,2	0,5	0,4	0,6	0,7	0,8	1,0	1,4	2,1	2,6	3,1	2,4	**1,3**
	b	-0,9	-2,5	-1,7	-1,6	-1,5	-1,0	-0,9	-1,1	-1,3	-1,5	-1,7	-2,0	-2,5	-2,9	-3,5	-2,4	**-1,8**
	c	1,0	1,1	1,1	1,0	1,0	1,0	1,0	1,0	1,0	1,0	1,0	1,0	1,1	1,1	1,2	1,1	**1,0**
	Error	0,05	0,82	0,23	0,14	0,28	0,36	0,40	0,74	0,64	0,49	0,33	0,25	0,10	0,14	1,26	0,51	**0,42**
CUBIC	a	-0,6	-0,4	0,5	-5,3	-1,5	-6,2	-5,6	-3,4	-2,8	-3,0	-3,1	-3,1	-2,5	-1,0	1,7	1,3	**-2,2**
	b	0,9	2,5	0,2	6,0	3,0	7,8	7,1	4,8	4,2	4,6	4,9	5,3	5,1	3,8	1,2	1,0	**3,9**
	c	-1,1	-2,7	-1,5	-2,9	-2,1	-3,2	-3,0	-2,4	-2,4	-2,7	-3,0	-3,2	-3,4	-3,2	-2,9	-2,0	**-2,6**
	d	1,0	1,1	1,0	1,1	1,1	1,1	1,1	1,0	1,1	1,1	1,1	1,1	1,1	1,1	1,1	1,1	**1,1**
	Error	0,05	0,82	0,23	0,11	0,27	0,20	0,23	0,67	0,59	0,42	0,26	0,18	0,07	0,13	1,25	0,50	**0,37**

From graphs, we observe that the points are distributed around a tendency curve. Applying the minimum square method (Arora [5]) for the several points $[M_{ki}/M_{ui}, w_i] \equiv (x_i, y_i)$ and approximating by the following functions:

$$\begin{aligned} &y = ax + b \quad - && \text{Linear} \\ &y = ax^2 + bx + c && \text{Quadratic} \\ &y = ax^3 + bx^2 + cx + d && \text{Cubic} \end{aligned} \tag{8}$$

we obtain the values of coefficients *a*, *b*, *c* and *d*. In Figs. 5 and 6 we show the tendencies obtained for the points of sections showed in Figs. 3 and 4.

Table 6 -- Values of *a*, *b*, *c* and *d* for sections solicited up to $0.8M_u$, for the 40 *m* long structure

Coefficients		Sections											Mean
		4	5	6	10	11	12	13	14	15	16	17	
LINE	a	-0,6	-0,7	-0,8	-0,6	-0,6	-0,5	-0,5	-0,5	-0,5	-0,5	-0,6	**-0,6**
	b	1,0	0,9	1,0	0,9	0,9	0,9	0,8	0,8	0,8	0,8	0,8	**0,9**
	Error	1,98	4,12	2,75	3,26	3,38	3,95	4,20	4,75	4,83	4,85	6,77	**4,08**
QUADRATIC	a	0,4	0,2	0,4	0,2	0,7	1,1	1,5	1,8	2,1	2,5	3,5	**1,3**
	b	-1,1	-0,9	-1,2	-0,8	-1,3	-1,7	-2,0	-2,2	-2,5	-2,9	-3,6	**-1,8**
	c	1,1	1,0	1,0	0,9	1,0	1,0	1,1	1,1	1,1	1,2	1,3	**1,1**
	Error	1,88	4,11	2,68	3,24	3,16	3,43	3,47	3,75	3,51	3,09	4,28	**3,33**
CUBIC	a	-1,6	-2,8	-1,7	-3,1	-2,2	-1,5	-1,6	-1,6	-1,7	-1,7	-1,4	**-1,9**
	b	3,1	4,9	3,2	5,0	4,1	3,5	3,8	4,2	4,5	4,9	5,3	**4,2**
	c	-2,3	-3,1	-2,5	-2,9	-2,7	-2,7	-2,9	-3,2	-3,4	-3,8	-4,3	**-3,1**
	d	1,2	1,2	1,2	1,1	1,1	1,2	1,2	1,2	1,2	1,3	1,3	**1,2**
	Error	1,74	3,62	2,52	2,93	2,99	3,35	3,41	3,69	3,46	3,04	4,26	**3,18**

The results obtained for sections that resisted at least $0.8M_u$ are shown in Table 5, for the 30 *m* long structure, and in Table 6, for the 40 *m* long structure. We considered the number $0.8M_u$ because usually the structures are designed to work until this bending moment value and so using these data we can obtain the curves up to values that really happen in practice. There are cases when special overloads not foreseen in design happens, as, for example, the shock of a vehicle, leading to bending moments values larger than M_u. It is very important to the designer to know the behavior of this kind of structures near to the failure, because he can explore this aspects to reinforce an existing structure, or to design a new structure.

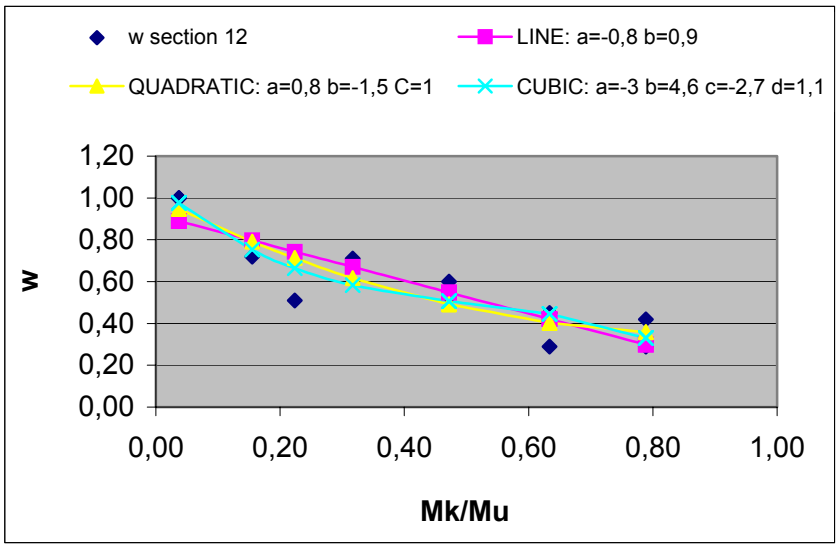

Fig. 5 -- Tendencies obtained for section 12 for the 30 *m* long structure

One should note that the sections where the largest stiffness loss was numerically obtained, section 17 for the 30 m long structure, and section 2 for the 40 m structure, were the sections that indeed collapsed in the tests. It is possible that this analysis methodology may be used as a "warning" that a certain section is the most probable to collapse. The formulation presented here is very useful to analyze the behavior of one specific section, especially in failure prevention and maintenance of structures. As we will show further on in this paper, the computation of the structure displacements using this formulation is not as precise as the one showed in next section.

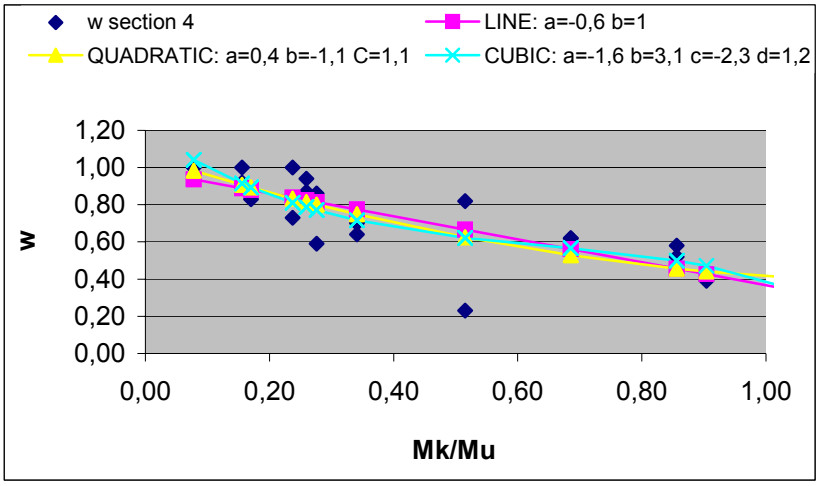

Fig. 6 -- Tendencies obtained for section 4 for the 40 *m* long structure

The mean values of coefficients *a*, *b*, *c* and *d* were determinate, as well as the mean value of the absolute quadratic error corresponding to each approximation function, as shown in Tables 5 and 6. For the three kinds of equations used, the linear equation presents the biggest approximation error with small variation of coefficients. The cubic equations presented the smallest approximation error, but its coefficients varied too much. The quadratic equations presented an intermediate behavior. Note that the approximation errors given by Tables 5 and 6 are those between the *w*'s curves and the *w*'s values obtained from the optimization problem defined in equations (5) and (6). So, this error is not the approximation error between the displacements measured in tests and those given by the integration of neutral line equation. In the next section, the error presented in Tables 7 to 12 are those between the displacements measured in tests and those given by the integration of neutral line.

4.2 Second Formulation – One Equation for Whole Section

Inspired in curves shown in previous section, we define some different optimization problems, in which we go straight to the coefficients of equations given in (8). Now the coefficients of these equations are the design variable of optimization problems. In this formulation we do not need to compute the values of

w, use least square method and obtain the values of *a*, *b*, *c* and *d* for each section. In the following algorithm we compute the coefficients of only one equation for the whole structure. It is easier to use in practice and, as we will see ahead, it gives us a more precise computation of the displacements.

The functions given in (8) represent the values of the effective stiffness parameter $w = y = g(a,b,...,e)$. In the formulation presented in this section, the coefficients of these functions are the design variable of optimization problems, while the objective function is the quadratic error between the displacements measured in tests and those given by the integration of neutral line deferential equation. So we will define three optimization problems, based on three design variable vectors:

$$\begin{aligned} &\boldsymbol{b} = \begin{bmatrix} a & b \end{bmatrix}^T - && \text{Linear} \\ &\boldsymbol{b} = \begin{bmatrix} a & b & c \end{bmatrix}^T && \text{Quadratic} \\ &\boldsymbol{b} = \begin{bmatrix} a & b & c & d \end{bmatrix}^T && \text{Cubic} \end{aligned} \tag{9}$$

Note that now for any section we have $w = w(\boldsymbol{b},x_{jk})$, where $\boldsymbol{b}$ is one of the vectors defined in (9) and $x_{jk} = M_{jk}/M_{uj}$, where M_{jk} is the bending moment acting on the *j*-th section at the *k*-th load step, and M_{uj} is the ultimate Code based bending moment of the *j*-th section computed according NBR-6118-03 (ABNT [3]) Brazilian Code. Using this definition, we consider now the value of the effective moment of inertia as

$$I_{EF}(z_j)_{,k} = w(\boldsymbol{b},x_{jk})\, I(z_i). \tag{10}$$

The quadratic error now is given by:

$$E_q(\boldsymbol{b}) = \frac{1}{2}\sum_j \sum_k \left[v(z_j, w(\boldsymbol{b}, x_{\boldsymbol{jk}})) - v_{r\,jk} \right]^2, \tag{11}$$

where $v(z_j, w(\boldsymbol{b}, x_{\boldsymbol{jk}}))$ is the numerical displacement, at the *j*-th section and at the *k*-th load step, computed using the effective stiffness given in (10) and the integration scheme given by (2). The matrix $v_{r\,jk}$ is the experimentally measured displacement at the *j*-th section at the *k*-th load step. For the 30 *m* long structure the matrix $v_{r\,jk}$ is shown in Table 3, while for the 40 *m* structure this matrix is shown in Table 4.

As we can see, the problem to minimize the approximation error (Eq. 11) consist of determining the vector $\boldsymbol{b}$ that gives the best approximation of the numerical displacements, matrix $v(z_j, w(\boldsymbol{b}, x_{\boldsymbol{jk}}))$, with the real experimentally measured displacements, matrix $v_{r\,jk}$. So, we can formulate the following optimization problem. Determine $\boldsymbol{b} \in \Re^l$, where *l* takes the values according to $\boldsymbol{b}$ defined in Eq. (9), that minimize the objective function

$$f(\boldsymbol{b}) = E_q(\boldsymbol{b}), \tag{12}$$

subjected to constrains:

$$w_s(z_i) \le w(\boldsymbol{b}) \le 1, \quad \text{para} \quad i = 0, 1, ..., n. \tag{13}$$

The first optimization problem solved using this formulation was applied to the 30 *m* long structure. We solved the problem considering only the 30 *m* long structure data, given in Table 3. For this structure we obtain the equations given in Table 7, while the graphs of these functions are shown if Fig. 7.

Table 7 -- Values of *a*, *b*, *c* and *d*, number of iterations and the approximation error for the whole structure, considering only the 30 *m* long structure (second formulation)

Equation	Coefficients of Equations				Iteractions	Error
	a	b	c	d		
Linear	-0,535268	0,740305	-	-	255	1495,78
Quadratic	1,129912	-1,861248	1,096291	-	36922	1199,06
Cubic	-1,571899	3,711060	-3,189166	1,306559	18	1225,34

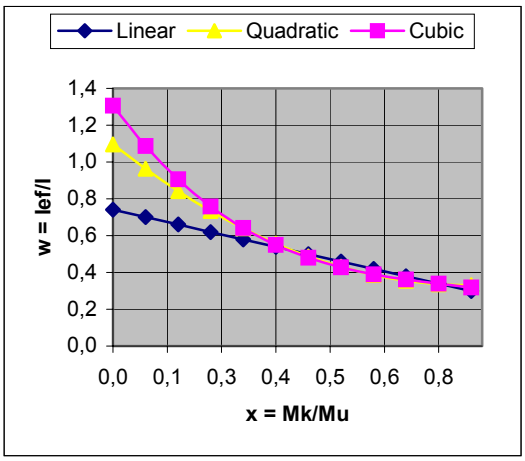

Fig. 7 -- Curves obtained considering only the 30 *m* long structure (second formulation)

In the second optimization problem we considered only the 40 *m* long structure data, given in Table 4. For this structure we obtain the equations given in Table 8, while the graphs of these functions are shown if Fig. 8.

Table 8 -- Values of *a*, *b*, *c* and *d*, number of iterations and the approximation error for the whole structure, considering only the 40 *m* long structure (second formulation)

Equation	Coefficients of Equations				Iteractions	Error
	a	b	c	d		
Linear	-0,390864	0,657959	-	-	81	8685,28
Quadratic	0,097746	-0,550895	0,716094	-	6450	8549,09
Cubic	-1,352466	3,071607	-2,469927	1,049532	19	8139,44

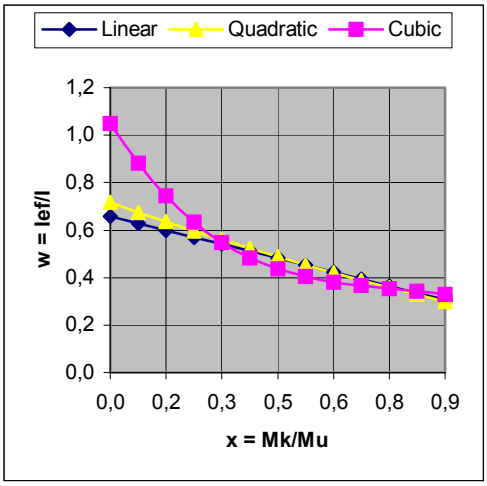

Fig. 8 -- Curves obtained considering only the 40 *m* long structure (second formulation)

The third optimization problem solved considered both the 30 and 40 *m* long structures. We found one solution that is the optimum considering the two structures. So we used data given in both Tables 3 and 4. The equations obtained are shown in Table 9, while the graphs of these functions are shown if Fig. 9.

Table 9 -- Values of *a*, *b*, *c* and *d*, number of iterations and the approximation error for the whole structure, considering both the 30 and 40 *m* long structures (second formulation)

Equation	Coefficients of Equations				Iteractions	Error 30m	Error 40m	Error Total
	a	b	c	d				
Linear	-0,389330	0,651252	-	-	94	2103,75	8196,32	10300,08
Quadratic	0,206218	-0,719639	0,770848	-	5310	1526,48	8357,40	9883,88
Cubic	-1,289704	3,037593	-2,597529	1,130748	20	1363,72	7631,48	8995,20

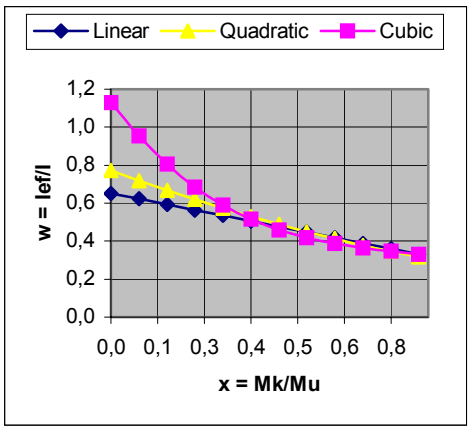

Fig. 9 -- Curves obtained considering both the 30 and 40 *m* long structures (second formulation)

Putting in a graph (Fig. 10) the cubic equation solution for the 30 *m* long structure, for the 40 *m* long structure, and for both structures, we can see that the

optimum of both structures lye between the two previous curves. At this point, some important questions are: should we consider the mean value equations given in Tables 5 and 6, or one equation for each section? How much would the error (Eq. 11) be? The performance would be better or worse than those presented in Tables 7 to 9? We computed the displacements and the respective errors considering these values. Considering one equation specific for each section, as given by Table 5 for 30 *m* structure and Table 6 for 40 *m* structure, we computed the approximation error given by Eq. 11. In case of both structures, for the sections that are not included in Tables 5 and 6 we considered the mean values of coefficients shown in the last column of those tables. It is important to remember that to compute the approximation error (Eq. 11) it is necessary to compute the structure nodal displacement for every load step and then compare these values with those experimentally measured.

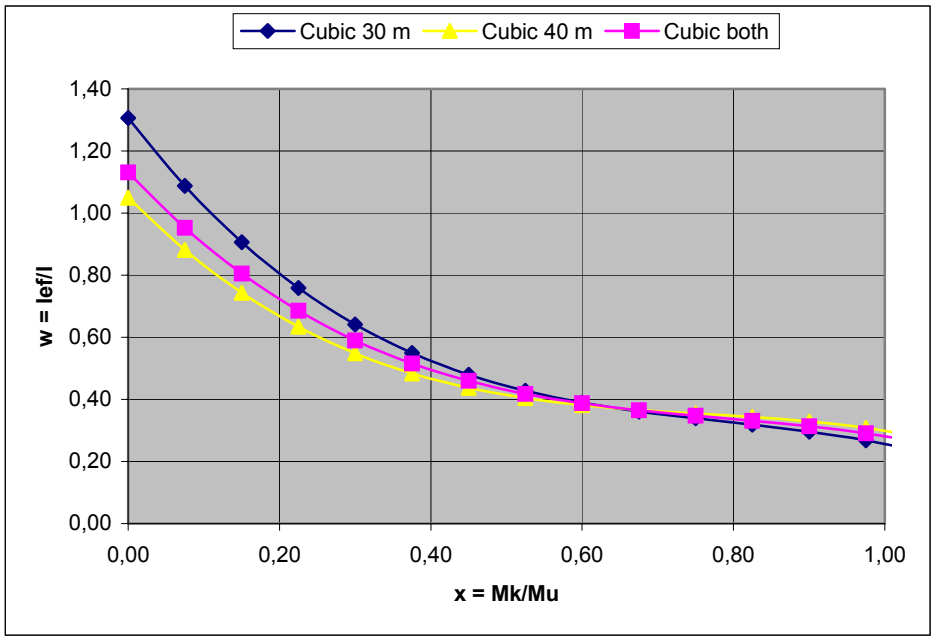

Fig. 10 -- The three cubic obtained: 30 *m* structure, 40 *m* structure and both structures (second formulation)

For both structures, the minimum approximation error was given by this second formulation, which is based in only one equation that represents all the structure behaviour. This procedure is much more efficient to compute the structures displacements. The values of Table 7 (30 *m* structure – second formulation, one equation for the whole structure) are up to 60% smaller than those computed for the 30 *m* structure, considering the first formulation with one equation for each section. The errors of Table 7 are also up to 40% smaller than those computed for the 30 *m* structure, considering the first formulation and using the mean value of coefficients of Table 3 (one equation) for the whole structure. Analysing the results of this work, we conclude that the quadratic equation shown in Table 7 provided the minimum error and consequently the best approximation of the effective stiffness for the 30 *m*

structure. In case of 40 m structure, the cubic equation given in Table 9 provides the minimum approximation error and consequently the best approximation of the effective stiffness.

Based on the results obtained in this section, specific for the structures and tests analysed here, we can conclude that the second formulation presented here render a better approximation of the displacements values, than the first formulation presented in the previous section. The second formulation gives one equation for the whole structure, while the first one gives one equation for each section. While the second formulation gives a better computation of structural displacements, it does not provide information about on specific section, as the first formulation provides. If we are interested in reinforcing an existing given structure, probably the first formulation is more interesting to be used, while if we are interested in computing the displacements or in designing a new structure, the second formulation is more useful.

Others important considerations here are related to the elasticity modulus of concrete. In this work we considered $E = 41.4$ *GPa*, computed according to NBR-6118-78 (ABNT [2]) Brazilian Code. This value is larger than values measured in tests, around 21 *GPa*, and larger than the value given by the revision of that Code, the new NBR-6118-03 (ABNT [3]), around 31.9 *GPa*. Tests accomplished using the formulation proposed here showed that when we solve the optimization problem and compute a certain function $w_1(x)$ considering a given elasticity modulus of concrete E_1 and solve the problem again using another value E_2, the new value of w is $w_2(x) = E_1 w_1/E_2$, in other words, the quantity $E_1 w_1 = E_2 w_2 = E_i w_i$ is a constant. In our case, the elasticity modulus measured in tests for the structures analyzed here is equal to 21 *GPa*, the coefficients a, b, c e d presented in this work must be multiplied by $41.4/21 = 2.0$ to get the correct values of coefficients. In practice, it is not necessary to compute displacements again, because if we use the effective stiffness concept, as we noted earlier, the product Ew stays constant and final results are the same.

5 Conclusions

In this work we have presented experimental work conducted on two 30 and 40 *m* above ground long structures. Data from tests were processed using optimization techniques to compute the effective stiffness of sections. We determined relationships between the effective bending stiffness and the bending moment value in a RC section. We presented two different formulations.

The first one provides one equation for each section of a discretized structure. This formulation can provide information specifically about one given section, and it makes possible to predict what section will probably collapse during a possible structure failure and what section is necessary to reinforce in case of existing similar structures reinforcement.

The second formulation presented here provides one equation that represents the behavior of the whole structure. This formulation is better to predict the displacements that will happen in a certain structure under a given loading and it is very helpful to compute correctly the displacements and, in case of designing a new structure, to predict the future behavior of a similar structure.

In both formulations, we used three different equations to represent the effective bending stiffness parameter. They are linear, quadratic and cubic equations. In most cases analyzed here the cubic provides the smaller approximation error, but the coefficients of the equations vary considerably from one type of structure to the other, or from one section to the other. Among these equations, the linear one usually provides the largest approximation error but the values of coefficients do not change much from one structure to other or from one section to other. We note that the equations for the 30 *m* structure, using the second formulation, is quite similar to the equations obtained for 40 *m* structure using the same formulation.

The conclusions presented here are based on the analysis of two 30 and 40 *m* long structures. These structures are flanged structures and, near to the flange, there are large concentrations of steel, what can make this kind of structure stiffer than others non flanged RC structures.

We suggest for future works to analyze several kind of structures, flanged and non flanged, to identify standard equations for each kind of structure. Additional suggestions for future work are:

i) search for a possible relationship between the coefficients of the approximation functions and the arrangements and properties of the RC sections;
ii) explore some aspects related to the theory of structural failure, searching for a relationship between the sections where the largest losses happen and the sections that indeed collapsed in real similar cases;
iii) instead of using equation (1), we intend to also use the exact curvature equation leading to equation $\frac{v''}{\sqrt{\left(1+v'^2\right)^3}} = -\frac{M_k(z)}{EI_{EF}(z)}$, accomplishing a geometrically nonlinear analysis;
iv) use other processes to integrate the neutral line equation, instead of (2);
v) in the experimental work, study the influences of the structure self-weight, the friction between the movable supports and steel plates on which they are mounted on and the stiffness of the structure support in the results obtained;
vi) define an optimization problem to minimize the cost of a Telecommunication Tower; use several different kind of *w*'s equations and analyze the sensitivity of the final design related to the coefficients of *w*'s equations.

Acknowledgments

This work was accomplished under a Project of Pos-Doctoral Apprenticeship sponsored by CAPES, a Brazilian agency for research, Project No. 0606-04-9. The research was completed when M. A. da Silva was a visiting scholar in the Department of Civil and Environmental Engineering of The University of Iowa from October to November 2004. A great part of the research was also done using resources of the Optimal Design Laboratory and The University of Iowa.

References

[1] ABNT – Associação Brasileira de Normas Técnicas, NBR-6123-87: Forças Devidas ao Vento em Edificações, 1987.

[2] ABNT – Associação Brasileira de Normas Técnicas, NBR-6118-78: Projeto e Execução de Obras de Concreto Armado, 1978.

[3] ABNT – Associação Brasileira de Normas Técnicas, NBR-6118-03: Projeto de Obras de Concreto, 2003.

[4] ACI – American Concrete Institute, ACI-318-71 - Building Code Requirements for Reinforced Concrete, Detroit, EUA, 1971.

[5] Arora, J. S., *Introduction to Optimum Design*, Second Edition, Elsevier Academic Press, 2004.

[6] Branson, D. E., Instantaneous and Time-Dependent Deflections of Simple and Continuous Reinforced Concrete Beams, Report Nº. 7, Alabama Highway Research Report, Bureau of Public Roads, Aug. 1963, pp. 1-78, 1963.

[7] Brasil, R. M. L. R. F. and Silva, M. A., Determination of Effective Bending Stiffness Using Optimization Techniques Applied To Experimental Results, XXV CILAMCE, Recife, Brazil, 2004.

[8] Brasil, R. M. L. R. F. and Silva, M. A., RC Large Displacements: Optimization Applied To Experimental Results, CST-2004, Lisbon, 2004.

[9] Chahande, A. I. and Arora, J. S., Optimization of large structures subjected to dynamic loads with the multiplier method, International Journal For Numerical Methods in Engineering, 37, pp. 413-430, 1994.

[10] Silva, M. A. and Brasil, R. M. L. R. F., Técnicas de Otimização Aplicadas a Resultados Experimentais no Estudo da Redução da Rigidez Flexional em Estruturas de Concreto Armado, Boletim Técnico da EPUSP, BT-PEF-0401, São Paulo, 2004.

[11] Silva, M. A. and Brasil, R. M. L. R. F., Nonlinear Dynamic Analysis Based on Experimental Results of RC Towers for Telecommunication Subjected to Wind Loading, DINCON2004 - 3º Congresso Temático de Dinâmica e Controle da SBMAC, Ilha Solteira, 2004b.